Progress In Electromagnetics Research, Vol. 137, 741–758, 2013

EFFICIENT NEURAL NETWORK APPROACH FOR 2D DOA ESTIMATION BASED ON ANTENNA ARRAY MEASUREMENTS

Marija Agatonović[1, *], Zoran Stanković[1], Ivan Milovanović[2], Nebojša Dončov[1], Leen Sit[3], Thomas Zwick[3], and Bratislav Milovanović[1]

[1]Faculty of Electronic Engineering, University of Niš, Niš 18000, Serbia

[2]Singidunum University, Belgrade 11000, Serbia

[3]Institut für Hochfrequenztechnik und Elektronik, Karlsruhe Institute of Technology, Karlsruhe 76131, Germany

Abstract—In this paper, we present an efficient Artificial Neural Network (ANN)-based model to estimate both azimuth and elevation arrival angles of a signal source. To achieve this goal, the ANN model is constructed using measurement data obtained by a rectangular antenna array in the space-frequency domain. Unlike classical super-resolution algorithms such as 2D MUSIC, the proposed model is capable to account for imperfections of measurement equipment as well as mutual couplings between array elements. The neural model has been verified for several angular positions and frequencies. It is shown that the use of ANN model to estimate angular positions of a signal source yields more accurate results when compared to 2D MUSIC. Moreover, the neural model significantly outperforms 2D MUSIC in terms of speed of computation.

1. INTRODUCTION

The concept of SDMA (Space Division Multiple Access) employs smart antennas and digital signal processing algorithms to increase the capacity of modern wireless communication systems. By exploiting the users' spatial separability, this multi-user access scheme has the ability to automatically sense and suppress interference while simultaneously enhancing desired signal reception [1]. The typical procedure of SDMA

Received 21 January 2013, Accepted 8 March 2013, Scheduled 12 March 2013

* Corresponding author: Marija Agatonović (magatonovic@gmail.com).

includes Direction of Arrival (DOA) estimation of users' signals and adaptive beamforming. Assuming that the antenna array manifold is known and all users are located in the far-field of the array, DOA estimation algorithms are used to retrieve the DOAs from the data of array output. Next, the adaptive beamforming is applied, so that the radiation pattern of the smart antenna is dynamically tuned to specific directions through complex weights adjustments. Consequently, users operating outside the bounds of the directed beams experience a near zero interference from other users operating under the same base station with the same radio frequency. This attribute of SDMA allows base stations to have larger radio coverage with less radiated energy. Also, the SDMA architecture saves on valuable network resources and prevents redundant signal transmission in areas where users are currently inactive.

So far, numerous algorithms have been devised to deal with the DOA estimation problem and among them, the subspace-based methods MUSIC (MUltiple SIgnal Classification) and ESPRIT (Estimation of Signal Parameters via Rotational Invariance Techniques), are best known for their super-resolution capabilities [2, 3]. Performing spectral search procedure, MUSIC is able to provide accurate DOA estimation at the expense of high computational complexity. When multidimensional parameter estimation is required, ESPRIT demonstrates significant advantage over MUSIC. Avoiding the orthogonally search, its computational complexity grows linearly with the dimension while that of MUSIC grows exponentially. Subsequently, for two-dimensional (2D) DOA estimation, MUSIC algorithm performs a spectrum peak search for all angles in azimuth and elevation what causes demanding computations, and makes this algorithm unsuitable for real-time user tracking. To overcome this problem a number of algorithms have been developed [4–16]. For 2D scenarios, ESPRIT algorithm is extended in [10], to provide both azimuth and elevation estimates. Since this method does not require complex search procedure and initialization, its computational complexity is twice that of 1D ESPRIT. Unitary ESPRIT of similar computational complexity is presented in [11]. In [12, 13], a technique that uses generalized Rayleigh ratio theory is proposed. By the factorization of the steering vector with respect to DOA and nuisance parameters a simple 1D-optimization procedure is needed for accurate DOA estimation. It is shown that performance of this method is comparable to 2D MUSIC for higher SNR values ($> 20\,\mathrm{dB}$) [13]. A propagator model that avoids the need for eigenvalue decomposition is presented in [14]. The model exploits different arrangements of L-shaped array to accurately estimate azimuth and elevation arrival angles, but assumes ideal elements and neglects mutual

couplings. Investigation of the 2D DOA estimation using two L-shape arrays is performed in [15]. In [16], an approach based on singular value decomposition of cross-correlation matrices demonstrated high accuracy in 2D DOA estimation.

However, although all the mentioned algorithms provide lower computational and storage cost than 2D MUSIC, they are still not fast enough to estimate angular positions of a radiating source in real-time. For that reason, an alternative approach based on artificial neural networks (ANNs) has been proposed in this paper. Neural networks are very convenient as a modeling tool since they have the ability to learn from presented data [17–21]. Compared to conventional signal processing algorithms that are mainly based on linear models, neural networks consider DOA estimation as approximation of highly nonlinear multidimensional function, or in other words, as a mapping between spatial covariance matrix of received signals from antenna elements and DOAs. There are many publications on ANNs in DOA estimation of both narrowband and wideband signals [22–31]. Most of them report results on Radial Basis Function Neural Network (RBF-NN) modeling to estimate DOAs in azimuth plane only, but there are also papers addressing two-dimensional DOA estimation [32–35]. In [32, 33], a RBF-MLP (Multi-Layer Perceptron) neural network based sectorisation models are proposed. The models are trained with the simulation data and have demonstrated the ability to provide high-resolution 2D DOA estimates. Here, the simulations assumed a uniform rectangular array composed of isotropic antenna elements and ideal propagation environment. An approach using MLP neural networks and only amplitude data from an L-shaped array is discussed and validated in [34]. In [35], 2D DOA estimates in a hemispherical space are provided using RBF neural networks and circularly polarized patch antennas placed on a concentric circle around the feed element.

In this work, an artificial neural network based (ANN) model is developed for 2D DOA estimation using rectangular antenna array geometry. Data for ANN training and testing are provided from measurements. This prevents the failure of mathematical models owing to mismatch between assumed and real environment. It will be shown that the ANN model accurately estimates azimuth and elevation of a radiating source (a transmitting antenna) at angular positions and frequencies that have not been used in the learning process. Taking into account real measurement conditions and imperfections of the measurement equipment such as geometrical inaccuracies in the manufacturing of the rectangular array and reflections in antenna feed cables and connectors, the ANN model is able to eliminate errors due to these effects. Also, it does not need additional calibration

of the receiving array to minimize mutual couplings between array elements [36–39]. This is a very important feature of the proposed model as the presence of mutual coupling distorts phase vectors of radiation sources and the eigenstructure of the covariance matrix. Moreover, ANN model is able to perform well even in case of frequency dependent mutual coupling. Finally, the main advantage of the ANN model in comparison to 2D MUSIC is its efficiency. The model performs DOA estimation in a matter of seconds and has been proven as very suitable for real-time application.

The paper is organized as follows. In Section 2, an introduction to the signal model is given. Section 3 briefly presents the theory behind Multi-Layer Perceptron Neural Networks (MLP-NNs). System configuration for DOA measurements is described in Section 4 followed by a data pre-processing procedure for MLP-NN modeling in Section 5. In Section 6, the performance of developed neural models is presented and results are analyzed. The training and test statistics are given as well as plots of predicted vs. actual angular positions of a signal source. Also, a comparison with 2D MUSIC algorithm is presented. Section 7, the Conclusion, summarizes the main results.

2. PROBLEM FORMULATION

A rectangular array of $M \times N$ sensors with inter-element spacing d is used to intercept signals transmitted by K sources at angles $[(\varphi_1, \theta_1), (\varphi_2, \theta_2), \ldots, (\varphi_K, \theta_K)]$. The array is located in the vertical yz plane of spherical coordinate system where sensors are uniformly arranged in y- and z-directions at mutual distance between adjacent elements $d = \lambda/2$ (λ is the wavelength of the impinging waves). Position of each sensor in the array is determined by its coordinates (m, n), where $m = 0, 1, 2, \ldots, M-1$, and $n = 0, 1, 2, \ldots, N-1$. Element located in the origin of the coordinate system $(m, n) = (0, 0)$, is chosen as the phase reference point. The signal received at each sensor is sampled into P distinct frequency bins within the designed bandwidth. The array output in the pth frequency bin can be represented as

$$\mathbf{x}(f_p) = \sum_{k=1}^{K} \mathbf{a}(\varphi_k, \theta_k; f_p) s_k(f_p) + \mathbf{n}(f_p) \tag{1}$$

where $s_k(\cdot)$ is the signal received from the kth source at the reference antenna element, $\mathbf{n}(\cdot)$ the uncorrelated noise data, and

$$\begin{aligned} \mathbf{a}(\varphi_k, \theta_k; f) \;=\; & \Big[1 \ldots e^{j(2\pi f/c)(dm \cos\theta_k \sin\varphi_k + dn \sin\theta_k)} \ldots \\ & e^{j(2\pi f/c)(d(M-1) \cos\theta_k \sin\varphi_k + d(N-1) \sin\theta_k)}\Big]^T \end{aligned} \tag{2}$$

denotes the $MN \times 1$ steering vector associated with the kth source, where $[\cdot]^T$ is the transpose operator. We write (1) in matrix form as

$$\mathbf{x}(f_p) = \mathbf{A}(\varphi, \theta; f_p)\mathbf{s}(f_p) + \mathbf{n}(f_p) \tag{3}$$

for $p = 1, 2, 3, \ldots, P$. $\mathbf{A}$ is a $MN \times K$ steering matrix whose columns are the steering vectors of the K signals impinging on the rectangular array

$$\mathbf{A}(\varphi, \theta; f_p) = [\mathbf{a}(\varphi_1, \theta_1; f_p), \ldots, \mathbf{a}(\varphi_K, \theta_K; f_p)] \tag{4}$$

and $\mathbf{s}(f_p)$ is a signal vector

$$\mathbf{s}(f_p) = [s_1(f_p), \ldots, s_K(f_p)]^T \tag{5}$$

Further, to determine the angular positions of sources from the observed data $\mathbf{x}(f)$ it is necessary to estimate space-frequency covariance matrix $\mathbf{R}_\mathbf{x}(f)$. The covariance matrix in the pth frequency bin is defined as

$$\mathbf{R}_\mathbf{x}(f_p) = E\left\{\mathbf{x}(f_p)\mathbf{x}(f_p)^H\right\} \tag{6}$$

where $[\cdot]^H$ denotes Hermitian operator, and E is the expectation operator. Combining Equations (3) and (6), we obtain

$$\mathbf{R}_\mathbf{x}(f_p) = \mathbf{A}(\varphi, \theta; f_p)\mathbf{R}_\mathbf{s}(f_p)\mathbf{A}^H(\varphi, \theta; f_p) + E\left\{\mathbf{n}(f_p)\mathbf{n}(f_p)^H\right\} \tag{7}$$

where

$$\mathbf{R}_\mathbf{s}(f_p) = E\left\{\mathbf{s}(f_p)\mathbf{s}(f_p)^H\right\} \tag{8}$$

is the source covariance matrix. In this formulation it is assumed that the source signals and noise are uncorrelated.

3. MLP NEURAL NETWORKS

A neural network is a system composed of many simple processing elements (neurons) operating in parallel. Neurons in an MLP neural network are organized into an input, an output as well as several hidden layers. Every neuron in each layer of the network is connected to every neuron in the adjacent forward layer, and no connections are permitted between the neurons belonging to the same layer. Each neuron is characterized by a transfer function and bias, and each connection between two neurons by a weight. An MLP neural network is configured for a specific application through a learning phase in which several known input/output mappings are used to determine the network parameters. Weights are adjustable, and are typically calculated by means of an adaptive algorithm combined with training examples (input-output signals) presented during the training (or learning) phase.

Input signals propagate gradually through the network from the input layer through the hidden layers up to the output layer. It follows that the output of the l-th layer, $\mathbf{Y}_l$, can be written as

$$\mathbf{Y}_l = F(\mathbf{W}_l \mathbf{Y}_{l-1} + \mathbf{B}_l) \tag{9}$$

where $\mathbf{Y}_{l-1}$ is the output the $(l-1)$-th layer, $\mathbf{W}_l$ is a weight matrix between $(l-1)$-th and l-th layer and $\mathbf{B}_l$ is a bias vector between $(l-1)$-th and l-th layer. Function F is the activation function of each neuron and it is linear for input and output layers and sigmoid (tan-sigmoid in the particular case)

$$F(u) = (1 - e^{-u})/(1 + e^{-u}) \tag{10}$$

for hidden layers (Fig. 1) [40]. Usually all inputs and outputs to the network are normalized to an internal representation between -1 and 1, and the output is then rescaled to match the range of the training data. The most known training procedure is the backpropagation algorithm and its modifications such as quasi-Newton or Levenberg-Marquardt (LM) algorithms [40]. The training process of a MLP network is as follows. First, input vectors are presented to the input neurons and output vectors are calculated. These output vectors are then compared to target values and errors are determined. Error derivatives are calculated and summed up for each weight and bias until the whole training set has been presented to the network. Further, they are used to update the weights and biases for neurons in the model. The training process proceeds until errors are lower than the prescribed values or until the maximum number of epochs (epoch — the whole training set processing) is reached.

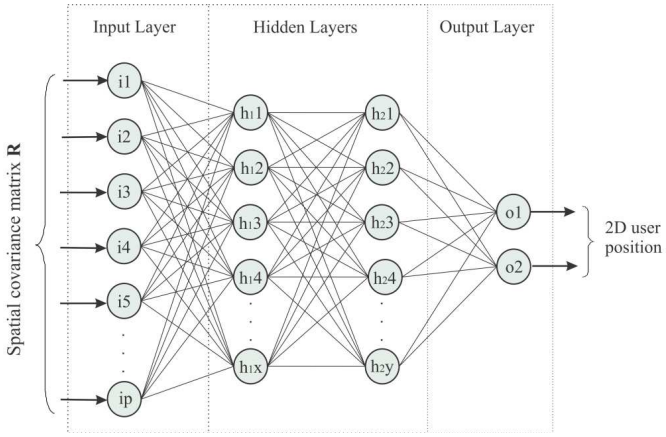

Figure 1. Multi-Layer Perceptron structure.

Once trained, the network is able to generalize that means, to perform well in response to input signals that have not been initially included in the training set. Generalizing performance of the trained MLP neural network can be expressed in terms of WCE (Worst Case Error), ACE (Average Case Error) or Pearson product-moment correlation coefficient, r, between reference values and network responses [40]. The formula for r is

$$r = \frac{\sum (x_i - \bar{x}_i)(y_i - \bar{y}_i)}{\sqrt{\sum (x_i - \bar{x}_i)^2 \sum (y_i - \bar{y}_i)^2}} \tag{11}$$

where x_i represents a reference value, y_i an ANN computed value, $\bar{x}$ a reference sample mean, and $\bar{y}$ an ANN sample mean. The correlation coefficient is an indicator of how well the modeled values match the actual ones. If the correlation coefficient is close to one then the neural network has an excellent predictive ability whereas r close to zero indicates poor performance of the network. Finally, the network architecture with the best performance is selected for further analysis.

4. SYSTEM SETUP

All the experimental works reported here were conducted in an anechoic chamber with dimensions of $7.44 \times 4.97 \times 4.69$ m. Since the chamber gives no possibility of generating multipath signals only the direct signal path between the transmitting (Tx) and receiving (Rx) antenna was considered (Fig. 2). The measurement system was based upon the classic vector network analyzer (VNA) technique. The VNA was used to measure the forward transmission scattering coefficient,

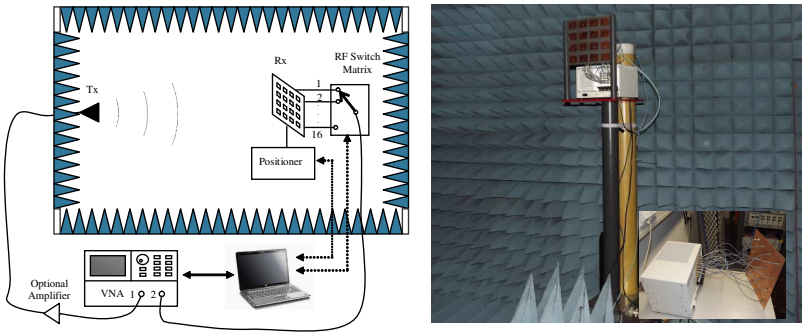

(a) (b)

Figure 2. (a) Measurement setup in the anechoic chamber, (b) receiving rectangular array on the antenna tower.

S_{21} (effectively the complex channel frequency response) [41]. A horn antenna was set to transmit a signal at the center frequency of 2.44 GHz. At the receiving site, a 4×4 rectangular microstrip patch array with a half-wavelength distance between adjacent elements was employed. Dimensions of microstrip patches were optimized in CST Microwave Studio, ($L = 39.6$ mm, $W = 49.4$ mm) and realized on a Duroid Rogers RT5880 substrate (epsilon = 2.2, thickness = 1.57 mm). The fabricated patch antennas resonated around 2.4400 GHz with a 10-dB bandwidth of approximately 60 MHz. Measured return loss of a single patch was −37 dB. HPBW (Half Power Beamwidth) of a single element was about 82.5° and measured gain was 6.7 dBi at resonant frequency.

The measurement procedure can be described as follows. The horn antenna and the array were placed at the same height (1.9 m), at two ends of the anechoic chamber so as to ensure that the array was in the far-field region of the horn antenna ($R = 5.1$ m). A HP 8510 VNA was used to measure the transfer function of the radio channel between two antennas. A RF switch was used to sample data from each array element. The switch matrix was placed on the antenna tower, behind the receiving array, and allowed each element of the array to be connected to each input of the switch matrix through a 40 cm long coax cable. In such a way, only one of the elements was active (ON) while the others acted as dummy elements. However, due to mutual couplings the other elements also radiated.

Once the measurement system was configured, antenna measurements were conducted in the anechoic chamber. Initially, the automated measurement system was calibrated and calibration data was saved separately from measurement data. These data were used later, in the process of 2D MUSIC algorithm validation. No calibration procedure regarding mutual coupling was performed. Received signals at rectangular array were sampled in a number of frequency points, and 2 snapshots (snapshot - sampling all the array elements) for each angular position of the transmitting antenna were recorded. The measurements at the VNA were averaged 16 times. The software in the chamber was upgraded in order to integrate RF switch matrix into the system. After that, the measurement system operated automatically and captured the data. Different positions in azimuth were obtained by rotating the antenna tower to a certain position in the region $[-45°, 45°]$, with the smallest step of $\Delta\varphi = 1°$.

Elevation angles were provided by changing the height of the tripod where the horn antenna was mounted ($\Delta h = 10$ cm). Measured signals for 19 elevation angles in the region $[-10°, 10°]$ were stored for further processing.

5. DIRECTION OF ARRIVAL ESTIMATION USING MLP NEURAL NETWORKS

Experimental data obtained from the 16-element rectangular array were utilized to estimate the space-frequency channel covariance matrix $\mathbf{R}$ (Fig. 3(a)). The matrix $\mathbf{R}$ was then used as input to an ANN developed to retrieve DOA of a source signal (Fig. 3(b)). In this work, we made a dimension-degraded training set to develop MLP-NNs as only the first row of a $MN \times MN$ covariance matrix was used to represent signals at the array output [23]. Further, keeping in mind that ANNs cannot operate with complex numbers, all ANN inputs were organized into a $2MN-1$ element vector $\mathbf{b}$. Before applied to the input layer of the neural network, the vector $\mathbf{b}$ was normalized (divided by its own norm), $\mathbf{z} = \mathbf{b}/\|\mathbf{b}\|$. So, the dimensionality of input vectors was significantly reduced allowing more efficient training of MLP-NNs. Finally, a database of training and test samples with the indexes of the transmitting locations was established.

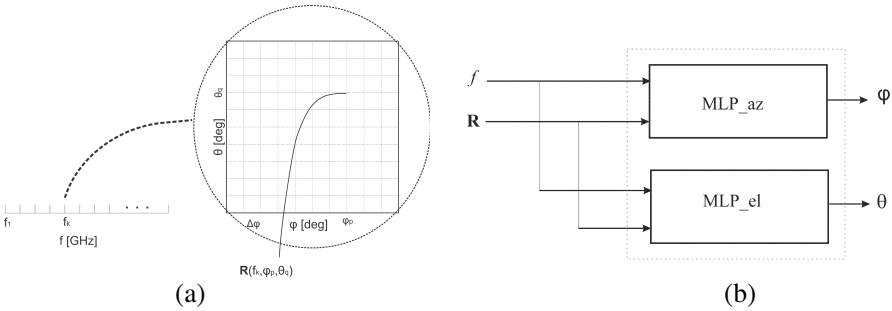

Figure 3. Illustration of (a) the training data structure, (b) the neural model for 2D DOA estimation.

6. MODELING RESULTS

As already mentioned in Section 4, to develop MLP-NN models for 2D DOA estimation, training and test sets were formed using experimental data. Training set was composed of 7905 samples for 31 azimuth angles from $-45°$ to $45°$ ($\Delta\varphi = 3°$), 15 elevation angles (0, ± 1.12, ± 3.36, ± 4.48, ± 5.6, ± 7.81, ± 8.92, ± 10), and 17 frequency points from 2.4100 GHz to 2.4700 GHz ($\Delta f = 3.6$ MHz). Similarly, the test set consisted of 868 samples, including 31 azimuth angles from $-45°$ to $45°$ ($\Delta\varphi = 3°$), 4 elevation angles (± 2.25, ± 6.71), and 7 frequency points. None of the test samples was used in the learning phase of MLP-NNs.

Further, a number of MLP neural networks with two hidden layers, aimed to separately estimate angular positions of the source in azimuth and elevation, were developed (Fig. 3(b)). The neural networks used both the frequency and spatial covariance matrix $\mathbf{R}$ as inputs, while the outputs were azimuth and elevation angles.

As the size of hidden layers in a network cannot be a priori known, the optimum number of neurons is usually found through an investigation. Namely, an iterative process is applied in order to dynamically adjust the network configuration. This procedure starts with a minimum network and then gradually adds hidden neurons and recalculates weights and biases during the training. As the iterative process converges to the solution, the network with good test statistics is obtained. If the number of hidden neurons is further increased (after an optimum configuration is found), the network will give excellent results for training samples but its generalization capabilities — results for test samples will be deteriorated due to overtraining. In Table 1, MLP-az_$H1$-$H2$ denotes MLP neural network model for azimuth estimates with $H1$ and $H2$ neurons in the first and second hidden layer, respectively, while MLP-el_$H1$-$H2$ denotes MLP network for elevation estimates.

Networks that have demonstrated the best test statistics, MLP_az-20-12 for azimuth, and MLP_el-16-12 for elevation, were utilized for further analysis. The appropriate correlation coefficient is 0.9997 for MLP_az-20-12 which has 20 and 12 neurons in two hidden layers, and 0.9987 for MLP_el-16-12 with 16 and 12 neurons in hidden layers. The response of the neural model (composed of two networks) for 2D DOA estimation is shown in Figs. 4–6. Correlation diagrams are plotted using the test data and illustrate the generalization capability of the neural model. In these figures, azimuth and elevation estimates are given for three test frequencies $f = 2.4220\,\text{GHz}$, $f = 2.4400\,\text{GHz}$ and $f = 2.4700\,\text{GHz}$ where grey dots represent MLP-NN responses and black dots denote results of 2D MUSIC algorithm. On the basis of these graphs, it can be concluded that the MLP-NN model exhibits slightly better performance than 2D MUSIC in the estimation of azimuth angles.

Also, we observe that MLP-NN demonstrates better ability to retrieve elevation angels, especially at the lower and higher frequencies of the operating band. Good results of MLP-NN model are consequence of its ability to account for real measurement conditions such as imperfections of measurement equipment and presence of systematic errors. Therefore, it is logical to expect better matching of the test and referent values with an already "known" measurement system (Table 2).

Table 1. Test statistics of MLP neural networks for DOA estimation of azimuth and elevation angles.

MLP_az			
Model	WCE (%)	ACE (%)	r
MLP_az-20-12	2.9848	0.8458	0.9997
MLP_az-25-15	3.0561	0.8725	0.9997
MLP_az-25-25	3.5554	0.9700	0.9997
MLP_az-22-18	3.8451	0.8244	0.9997
MLP_az-36-16	4.0394	0.8831	0.9997
MLP_az-19-17	5.3236	1.0067	0.9996
MLP_el			
Model	WCE (%)	ACE (%)	r
MLP_el-16-12	6.3149	1.6078	0.9987
MLP_el-21-17	6.4592	1.7025	0.9985
MLP_el-12-10	7.3799	1.8137	0.9984
MLP_el-22-18	7.1875	1.8197	0.9983
MLP_el-40-18	8.1340	1.8481	0.9983
MLP_el-20-12	8.0346	1.8645	0.9982

Table 2. Average error in estimating the transmitting antenna angular positions using MLP neural model and 2D MUSIC algorithm.

f [GHz]	MLP neural model		2D MUSIC	
	$\varphi_{\text{average error}}$ [deg]	$\theta_{\text{average error}}$ [deg]	$\varphi_{\text{average error}}$ [deg]	$\theta_{\text{average error}}$ [deg]
2.4112	0.7319	0.1942	3.7116	2.5406
2.4220	0.7019	0.1897	3.1604	2.2316
2.4304	0.7526	0.2149	2.2304	1.1860
2.4400	0.8274	0.2470	1.5511	1.0840
2.4508	0.8424	0.2301	1.7275	0.9740
2.4604	0.7536	0.2145	1.8697	1.6289
2.4700	0.7186	0.2200	2.1597	2.6233

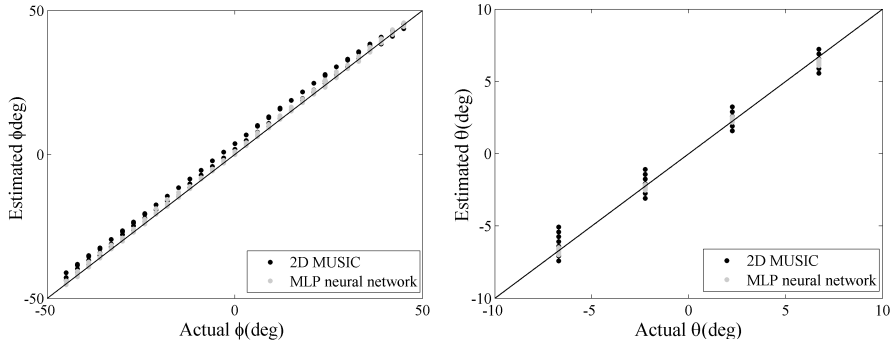

Figure 4. Scattering diagrams of the MLP neural network and 2D MUSIC azimuth estimates at test frequency $f = 2.4220\,\text{GHz}$.

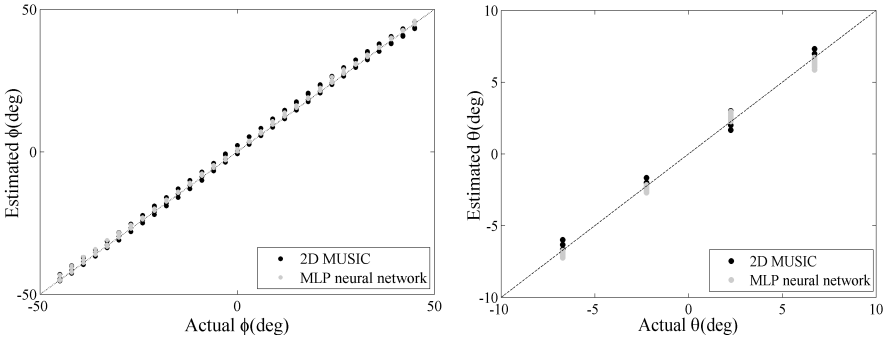

Figure 5. Scattering diagrams of the MLP neural model and 2D MUSIC elevation estimates at test frequency $f = 2.4400\,\text{GHz}$.

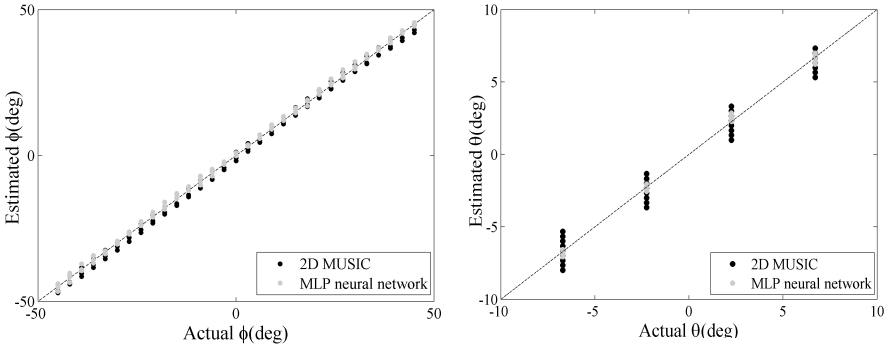

Figure 6. Scattering diagrams of the MLP neural model and 2D MUSIC elevation estimates at test frequency $f = 2.4700\,\text{GHz}$.

In Fig. 7, the root mean-square error (RMSE) in degrees is obtained across different frequency points, for all angular positions from both the training and test set. RMSE is calculated using the following expression

$$\text{RMSE} = \sqrt{E\left\{(\varphi_{ref} - \varphi_{est})^2 + (\theta_{ref} - \theta_{est})^2\right\}} \tag{12}$$

where φ_{ref} is the reference azimuth angle of the incoming signal, φ_{est} an azimuth estimate, and θ_{ref} a reference elevation angle of the signal while θ_{est} stands for an elevation estimate. As demonstrated in Fig. 6, MLP-NN has similar performance within the frequency band where RMSE, even in the worst case, does not exceed 2°. Estimation errors in these diagrams are mostly consequence of non-perfect alignment of antennas during the measurements in different measurement scenarios. In addition, frequency dependency of estimation error for three azimuth positions $\varphi_1 = -45°$, $\varphi_2 = 0°$ and $\varphi_3 = 45°$, and four elevation angles for each of them $\theta_1 = -6.72°$, $\theta_2 = -2.24°$, $\theta_3 = 2.24°$, $\theta_4 = 6.72°$, is plotted in Fig. 8. It can be seen that RMSE for all test positions has values in the range of [0.01°, 2°].

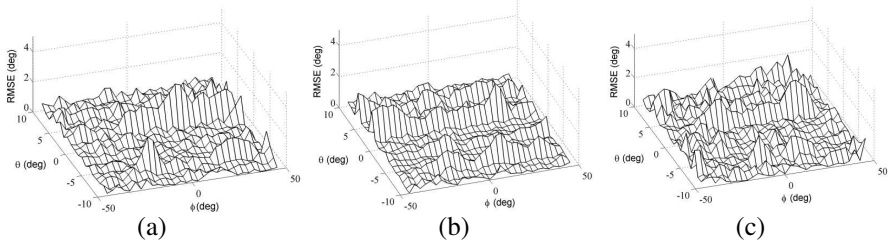

Figure 7. Root Mean Square Error (RMSE) of MLP-NN estimates at (a) $f = 2.4100\,\text{GHz}$, (b) $f = 2.4400\,\text{GHz}$ and (c) $f = 2.4700\,\text{GHz}$.

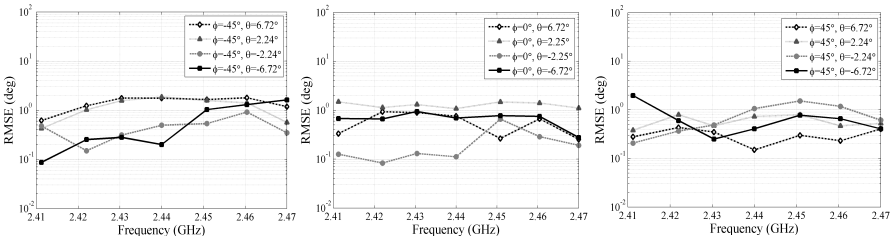

Figure 8. Frequency dependency of RMSE of estimated azimuth and elevation angles for several positions of the transmitting antenna.

The spectral search complexity of the conventional MUSIC-based algorithms is too high for real-time applications. The advantage of our MLP neural network model is the reduction in the processing time compared to the 2D MUSIC-DOA estimation. Here, we compare the processing time of the proposed model and the 2D MUSIC for our implementation in Matlab 7.10 on an Intel(R) Core(TM)2 Quad CPU computer running at 2.33 GHz. The simulation conditions were set to $\varphi = 36^\circ$ and $\theta = 8.92^\circ$, while the 2D MUSIC searching grid intervals in azimuth and elevation angles were set to 0.25°. We measured the propagation time of the MLP-NN model, presented in Fig. 3(a). After that, we used the same test pattern and measured the time required for the 2D MUSIC-DOA estimation. The processing time was 20 ms for the MLP-NN response and 17.8 s for the 2D MUSIC-DOA estimation in average.

7. CONCLUSION

In this paper, we have presented an efficient neural network-based model for estimation of 2D arrival angles. All geometrical inaccuracies in the manufacturing of the rectangular array as well as real measurement conditions and imperfections of the measurement equipment are comprised by the developed ANN model. The model eliminates errors due to reflections in cables and connectors, and does not need additional calibration procedure of the array to minimize effects of mutual couplings between array elements. It is shown that the neural model outperforms 2D MUSIC algorithm in terms of speed of computation. The efficiency of the ANN model stems from the fact that, after the learning phase, the directions of arrival are estimated with less memory requirements, since no 1D or 2D spectrum search is needed. Being able to provide fast and accurate 2D DOA estimates, the ANN model represents a promising solution for real time user tracking.

ACKNOWLEDGMENT

This work was supported by the project TR-32052 of the Serbian Ministry of Education and Science, and the project CARE (Coordinating the Antenna Research in Europe) of the Institut für Hochfrequenztechnik und Elektronik of the Karlsruhe Institute of Technology (KIT).

REFERENCES

1. Yang, J., X. Wu, and Q. Wang, "Channel parameter estimation for scatter cluster model using modified MUSIC algorithm," *International Journal of Antennas and Propagation*, Vol. 2012, 1–6, 2012.
2. Schmidt, R., "Multiple emitter location and signal parameter estimation," *IEEE Transactions on Antennas and Propagation*, Vol. 34, 276–280, 1986.
3. Roy, R. and T. Kailath, "ESPRIT-estimation of signal parameters via rotational invariance techniques," *IEEE Transactions on Acoustics, Speech and Signal Processing*, Vol. 37, 984–995, 1989.
4. Pouramadi, M., M. Nakhkash, and A. A. Tadion, "Application of MDL criterion for microwave imaging by music algorithm," *Progress In Electromagnetics Research B*, Vol. 40, 261–278, 2012.
5. Gu, X. and Y. Zhang, "Resolution threshold analysis of MUSIC algorithm in radar range imaging," *Progress In Electromagnetics Research B*, Vol. 31, 297–321, 2011.
6. Solimene, R., A. Dell'Aversano, and G. Leone, "Interferometric time reversal music for small scatterer localization," *Progress In Electromagnetics Research*, Vol. 131, 243–258, 2012.
7. Lee, J.-H., Y.-S. Jeong, S.-W. Cho, W.-Y. Yeo, and K. S. J. Pister, "Application of the Newton method to improve the accuracy of toa estimation with the beamforming algorithm and the MUSIC algorithm," *Progress In Electromagnetics Research*, Vol. 116, 243–258, 2011.
8. Bencheikh, M. L. and Y. Wang, "Combined ESPRIT-Root MUSIC for DOA-DOD estimation in polarimetric bistatic MIMO radar," *Progress In Electromagnetics Research Letters*, Vol. 22, 109–117, 2011.
9. Jiang, J.-J., F.-J. Duan, and J. Chen, "Three-dimensional localization algorithm for mixed near-field and far-field sources based on esprit and music method," *Progress In Electromagnetics Research*, Vol. 136, 435–456, 2013.
10. Kedia, V. S. and B. Chandna, "A new algorithm for 2-D DOA estimation," *Signal Processing*, Vol. 60, 325–332, 1997.
11. Jiang, J. and L. Gan, "Decoupled unitary esprit algorithm for 2-d DOA estimation," *Progress In Electromagnetics Research C*, Vol. 29, 219–234, 2012.
12. Ferreol, A., E. Boyer, and P. Larzabal, "Low cost algorithm for some bearing estimation methods in presence of separable nuisance parameters," *Electronics Letters*, Vol. 40, 966–967, 2004.

13. Hou, Y. S., J. Yong, and L. J. Zhang, "Low cost algorithm for azimuth-elevation joint estimation, 9th International Conference on Signal Processing," *Proceedings of the 9th Conference on Signal Processing ICSP*, 92–95, 2008.
14. Tayem, N. and H. M. Kwon, "L-shaped 2-dimensional arrival angle estimation with propagator method," *IEEE Transactions on Antennas and Propagation*, Vol. 53, 1622–1630, 2005.
15. Liang, J. and D. Liu, "Two l-shaped array-based 2-d DOAs estimation in the presence of mutual coupling," *Progress In Electromagnetics Research*, Vol. 112, 273–298, 2011.
16. Gan, L., J.-F. Gu, and P. Wei, "Estimation of 2-D DOA for noncircular sources using simultaneous SVD technique," *IEEE Antennas and Wireless Propagation Letters*, Vol. 7, 385–388, 2008.
17. Stankovic, Z., B. Milovanovic, and N. Doncov, "Hybrid empirical-neural of loaded microwave cylindrical cavity," *Progress In Electromagnetics Research*, Vol. 83, 257–277, 2008.
18. Wefky, A. M., F. Espinosa, L. D. Santiago, A. Gardel, P. Revenga, and M. Martinez, "Modeling radiated electromagnetic emissions of electric motorcycles in terms of driving profile using mlp neural networks," *Progress In Electromagnetics Research*, Vol. 135, 231–244, 2013.
19. Zaharis, Z. D., K. A. Gotsis, and J. N. Sahalos, "Adaptive beamforming with low side lobe level using neural networks trained by mutated Boolean PSO," *Progress In Electromagnetics Research*, Vol. 127, 139–154, 2012.
20. Luo, M. and K.-M. Huang, "Prediction of the electromagnetic field in metallic enclosures using artificial neural networks," *Progress In Electromagnetics Research*, Vol. 116, 171–184, 2011.
21. O'Halloran, M., B. McGinley, R. C. Conceicao, F. Morgan, E. Jones, and M. Glavin, "Spiking neural networks for breast cancer classification in a dielectrically heterogeneous breast," *Progress In Electromagnetics Research*, Vol. 113, 413–428, 2011.
22. El Zooghby, A. H., C. G. Christodoulou, and M. Georgiopoulos, "A neural network-based smart antenna for multiple source tracking," *IEEE Transactions on Antennas and Propagation*, Vol. 48, 768–776, 2000.
23. Çaylar, S., K. Leblebicioglu, and G. Dural, "A new neural network approach to the target tracking problem with smart structure," *Proceedings of the IEEE AP-S International Symposium and USNC/URCI Meeting*, 1121–1124, 2006.
24. Kim, Y. and H. Ling, "Direction of arrival estimation of humans

with a small sensor array using an artificial neural network," *Progress In Electromagnetics Research B*, Vol. 27, 127–149, 2011.

25. Wang, M., S. Yang, S. Wu, and F. Luo, "A RBFNN approach for DOA estimation of ultra wideband antenna array," *Neurocomputing*, Vol. 71, 631–640, Elsevier, 2008.
26. He, H., T. Li, T. Yang, and L. He, "Direction of arrival (DOA) estimation algorithm based on the radial basis function neural networks," *Advances in Intelligent and Soft Computing*, Vol. 128, 389–394, 2011.
27. Sarevska, M., B. Milovanovic, and Z. Stankovic, "Alternative signal detection for neural network based smart antenna," *Proceedings of the 7th Symposium on Neural Networks Application in Electrical Engineering, NEUREL*, 85–89, 2004.
28. El Zooghby, A. H., C. G. Christodoulou, and M. Georgiopoulos, "Performance of radial basis function networks for direction of arrival estimation with antenna arrays," *IEEE Transactions on Antennas and Propagation*, Vol. 45, 1611–1617, 1997.
29. Le, Z., "Research on direction of arrival estimation algorithm in smart antenna," Ph.D. Thesis, South China University of Technology, Guangzhou, China, 2010.
30. Zhang, Y., Z. Gong, and Y. Sun, "DOA estimation in smart antenna based on general regression neural network," *Journal of Military Communications Technology*, Vol. 28, 23–25, 2007.
31. Sarevska, M., B. Milovanovic, and Z. Stankovic, "Reliability of the hidden layer in neural network smart antenna", *WSEAS Transaction on Communications*, Vol. 4, 556–563, 2005.
32. Agatonovic, M., Z. Stankovic, and B. Milovanovic, "High resolution two-dimensional DOA estimation using artificial neural networks," *Proceedings of the 6th European Conference on Antennas and Propagation, EUCAP*, 1–5, 2012.
33. Agatonovic, M., Z. Stankovic, N. Doncov, L. Sit, B. Milovanovic, and T. Zwick, "Application of artificial neural networks for efficient high-resolution 2D DOA estimation," *Radioengineering*, Vol. 21, 1178–1186, 2012.
34. Jorge, N., G. Fonseca, M. Coudyser, J.-J. Laurin, and J.-J. Brault, "On the design of a compact neural network-based DOA estimation system," *IEEE Transactions on Antennas and Propagation*, Vol. 58, 357–366, 2010.
35. Matsumoto, T. and Y. Kuwahara, "2D DOA estimation using beam steering antenna by the switched parasitic elements and RBF neural network," *Electronics and Communications in Japan*

(Part I: Communications), Vol. 89, 22–31, 2006.

36. Zhou, Q.-C., H. Gao, F. Wang, and J. Shi, "Modified DOA estimation methods with unknown source number based on projection pretransformation," *Progress In Electromagnetics Research B*, Vol. 38, 387–403, 2012.
37. Kim, K. and T. K. Sarkar, "Direction-of-arrival (DOA) estimation using a single snapshot of voltages induced in a real array operating in any environment," *Microwave and Optical Technology Letters*, Vol. 32, 335–340, 2002.
38. Liao, W.-J., S.-H. Chang, H.-C. Liu, L.-K. Li, C.-Y. Hsieh, and C.-C. Yao, "A beam switching array antenna for direction-of-arrival applications," *Microwave and Optical Technology Letters*, Vol. 53, 1601–1606, 2011.
39. Cheng, S.-C. and K.-C. Lee, "Reducing the array size for DOA estimation by an antenna mode switch technique," *Progress In Electromagnetics Research*, Vol. 131, 117–134, 2012.
40. Zhang, Q. J. and K. C. Gupta, *Neural Networks for RF and Microwave Design*, Artech House, Norwood, MA, USA, 2000.
41. Randazzo, A., M. A. Abou-Khousa, M. Pastorino, and R. Zoughi, "Direction of arrival estimation based on support vector regression: Experimental validation and comparison with MUSIC," *IEEE Antennas and Wireless Propagation Letters*, Vol. 6, 379–382, 2007.